

IN SITU THICKNESS MONITOR FOR CONDUCTING FILMS

Sanjay A. Khan, James B. Farmer, Ronald J. Gutmann and Jose M. Borrego

Electrical, Computer and Systems Engineering Department and
Center for Integrated Electronics
Rensselaer Polytechnic Institute

Abstract: In-situ monitoring and control are desirable to improve yield in advanced IC fabrication processes. In this paper we propose a novel way to monitor the thickness of conducting films in-situ using a microwave reflection technique. We present results indicating the feasibility of our approach and discuss the design of the probe.

Introduction: Fabrication of VLSI chips involves the deposition and etching of conducting films with thicknesses ranging from 100 \AA for adhesion promoters/diffusion barriers upto several microns for high conductivity films. In general, the extent to which such a film reflects an incident electromagnetic wave is a function of its thickness, its conductivity, the frequency of the wave and the substrate on which the film is deposited. The dependence of the return loss on these parameters are studied using simulations for normally incident, plane electromagnetic waves in order to show the conductivity and thickness regimes where high sensitivity is expected in the 4-80GHz spectrum.

A schematic diagram of the model used in the simulations is shown in Figure 1. A free space plane wave is incident on a 25mil thick sheet of $10\Omega\text{-cm}$ Si which has a thin coating of metal on one side. The wave impedance to the right of the metal film is transformed through it and the silicon sheet to give the impedance seen by a plane wave at AA'. The return loss is then computed for different metal film sheet resistances and wave frequencies.

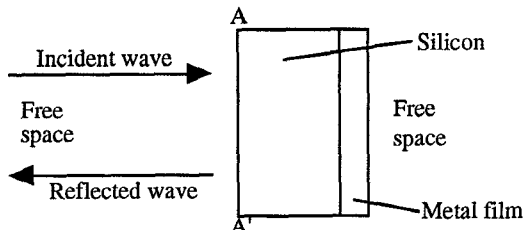
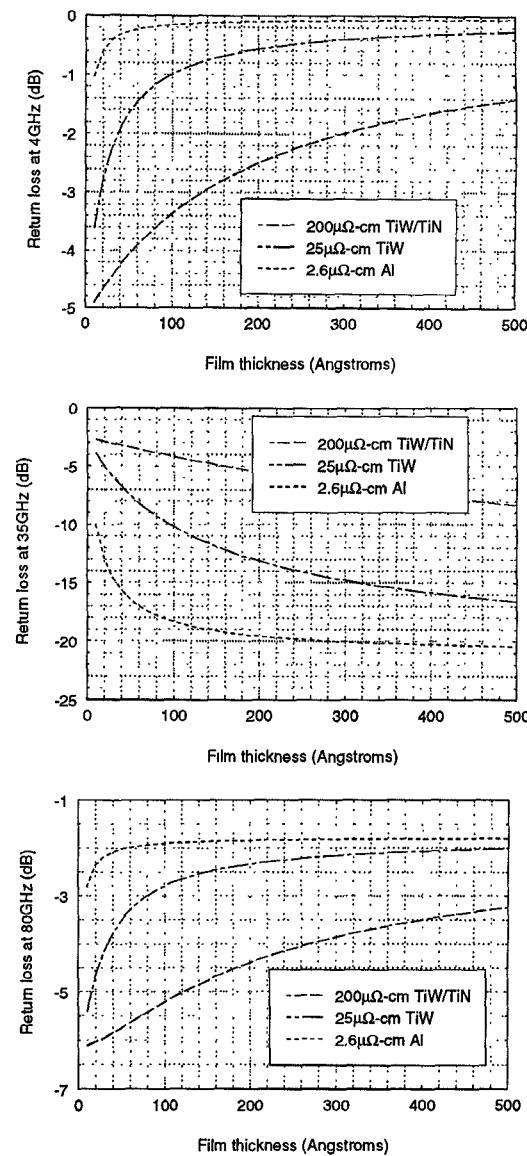


Figure 1:Schematic diagram of simulation model

Simulation results at 4, 35 and 80GHz are shown in Figure 2. The substrate resistivity is taken to be representative of a typical VLSI wafer, Aluminum represents a typical high conductivity film while Titanium/Tungsten and Titanium Nitride are representative of a typical adhesion promoter. Limiting resistivities of 25 and $200\mu\Omega\text{-cm}$ for TiW/TiN are used in the simulations since their thin film resistivities vary in this range depending on the deposition conditions [1].

Figure 2: Simulated plane-wave return loss versus film thickness at different frequencies - Si substrate resistivity = $10\Omega\text{-cm}$ in all cases

SS

Sensitivity is seen to be high ($>0.1\text{dB}/10\text{A}^\circ$ at 4GHz) in the 100A° regime for the low conductivity films, with enhanced sensitivity at 35GHz resulting from the 25mil Si substrate behaving like a quarter wave transformer at that frequency. While it may be difficult to monitor the deposition of thick ($>200\text{A}^\circ$), high conductivity films in the 4-80GHz frequency spectrum, a broadband probe designed in this range is expected to be useful for etch endpoint detection of such films. Moreover, such a probe should be very useful in the in-situ thickness monitoring of thin, high resistivity adhesion layers used in VLSI. A prototype of such a probe (essentially a broadband antenna with a balanced feed) is shown in Figure 3.

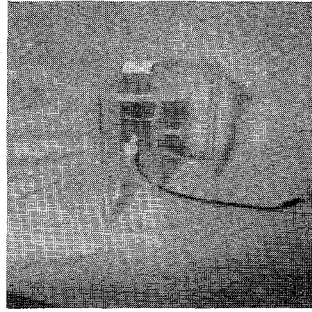


Figure 3: Model of substrate holder in a deposition/etch tool "under" which the probe is mounted. The probe dimensions are $3'' \times 1'' \times 1''$.

Design and Fabrication: A) The Antenna: Upon considering various antennas for use in the probe (including short electric and magnetic dipoles, Yagi-end-fire antennas and microstrip patch elements), the equiangular spiral antenna was deemed most appropriate for the following reasons:

- Its very high bandwidth, which is based on the simple fundamental principle that if the shape of the antenna be such that it can be specified entirely by angles, its performance would be independent of wavelength [2]. In principle, the arms of any such antenna will extend to infinity, but in practice, if the arm-length is equal to a wavelength at the lowest frequency of operation, performance essentially independent of frequency may be obtained.
- A full-wave arm can be spiraled into a diameter much smaller than its length, thus improving the resolution of the probe. This consideration is not important for monitoring the thickness of the first metal layer deposited in a fabrication process. For subsequent metallization steps, all patterned conducting layers below the one being deposited may influence the measurements. Since it may therefore be necessary to dedicate some real estate on the wafer for just this diagnostic, a smaller area of illumination is desirable.

Figure 4 shows a full wavelength spiral antenna (Min. Freq. of operation = 4GHz) printed on a gold-plated alumina wafer. If one of the conducting spirals is defined by the radius vectors

$$\rho_1 = ke^{a\phi}$$

$$\rho_2 = ke^{a(\phi - \delta)} = K\phi_1,$$

then the other spiral is defined by

$$\rho_3 = ke^{a(\phi + \pi)}$$

$$\rho_4 = K\phi_3.$$

"a" and " δ " are parameters that define the distance from the center to the farthest point away from the center on the spiral. In other words, "a" and " δ " must be chosen so that the "footprint" of the antenna is as small as possible, yet allowing the size and separation of the square pads near the center of the spiral to be large enough that it be practically feasible to feed it with a standard flexible coaxial cable via a suitable balun transformer.

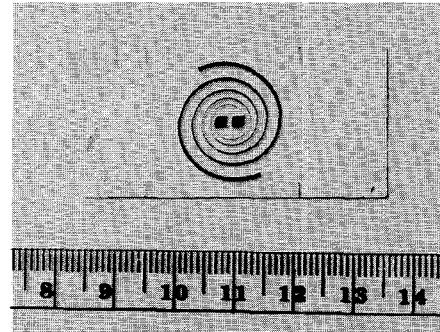


Figure 4: An equiangular spiral antenna fabricated on gold-plated alumina - min. freq. of operation = 4GHz (Scale in cm)

From reference [2], the radiation pattern and input impedance of the antenna are expected to be essentially constant over a 20:1 bandwidth for the full-wave antenna. The radiated E-field is circularly polarized and the radiation resistance decreases gradually as the spirals are made tighter (which can also be done by adjusting the size and spacing between the square pads near the center of the antenna shown in Figure 4). The pads were designed to be $2\text{mm} \times 2\text{mm}$ square with a separation of 0.636mm. Extrapolating the data from reference [2], this gives a radiation resistance of approximately 45Ω in free space.

B) The Balanced Feed: The balanced antenna cannot be directly fed by an unbalanced coaxial cable due to the possibility of exciting mast modes. A broadband balun transformer is therefore designed to gradually transform the coaxial cable into a two-wire transmission line. A way to achieve a broadband taper was suggested by Duncan, et al, [3] and is illustrated in Figure 5.

The impedance of the line changes depending upon how much of the outer conductor is cut. If the angle subtended by the cut at the center is 2α , the upper and lower bounds of the impedance are given as follows:

$$Z_{0(\text{upper})} = \frac{1}{2\pi} \sqrt{\frac{\mu}{\epsilon}} \ln\left(\frac{b}{a}\right) + \frac{\sqrt{\frac{\mu}{\epsilon}}}{\pi(\pi\alpha)^2} \sum_{n=1}^{\infty} \frac{\sin^2(n\alpha)}{n \left[1 + \coth\left(n \ln\left(\frac{b}{a}\right)\right) \right]},$$

where,

$$C_1 = \frac{\sum_{n=1}^{\infty} \frac{\sin^2(n\alpha)}{n(n^2 - k^2) \left[1 + \coth\left(n \ln\left(\frac{b}{a}\right)\right) \right]}}{\sum_{n=1}^{\infty} \frac{n \sin^2(n\alpha)}{(n^2 - k^2) \left[1 + \coth\left(n \ln\left(\frac{b}{a}\right)\right) \right]}}$$

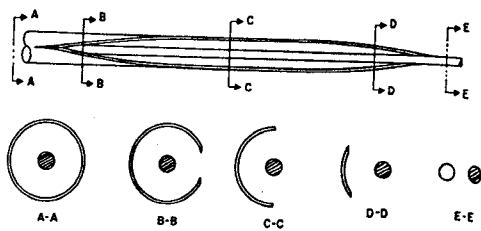


Figure 5: Coaxial to balanced two-wire taper

a = Diameter of inner conductor

b = Inner diameter of outer conductor;

$$Z_{0(\text{Lower})} = \frac{1}{2\pi} \sqrt{\frac{\mu_0 h(b)}{\epsilon_0 a^2}} \cdot \frac{1 - \frac{4}{5} \left(\frac{a}{b}\right) C_2}{1 - \frac{4}{5} \left(\frac{a}{b}\right) C_2}$$

where,

$$\frac{1}{C_2} = \frac{4}{5} \left(\frac{a}{b}\right) + \frac{40}{\pi} \ln \left(\frac{b}{a}\right) \sum_{n=1}^{\infty} \left[\frac{1 + \coth \left[n \ln \left(\frac{b}{a} \right) \right]}{n \alpha} \right] \frac{[A_n \cos(n \alpha) - B_n \sin(n \alpha)]^2}{(n \alpha)^4},$$

$$A_n = (n \alpha)^3 - 6(n \alpha) \text{ and}$$

$$B_n = 3(n \alpha)^2 - 6.$$

Since the impedance value was simply taken as the average of $Z_{0(\text{Upper})}$ and $Z_{0(\text{Lower})}$, the margin of error in the impedance for our design was about 7%.

All tapers were performed using a Klopfenstein taper [4]. The performance of this taper is optimum in the sense that for a given taper length the input reflection coefficient has minimum magnitude throughout the pass band, and for a specified tolerance of the reflection coefficient magnitude the taper has minimum length. For a taper of length "l" with Z_1 and Z_2 , the respective impedances at the two ends, the variation of the impedance for $-1/2 < x < 1/2$ is given by:

$$\ln(Z_0) = \frac{1}{2} \ln(Z_1 Z_2) + \frac{\rho_0}{\cosh(A)} \left[A^2 \phi \left(\frac{2x}{l} A \right) + U \left(x - \frac{l}{2} \right) + U \left(x + \frac{l}{2} \right) \right],$$

where,

U is the unit step function,

$$\phi(zA) = \int_0^z dy \frac{I_0(A\sqrt{1-y^2})}{A\sqrt{1-y^2}},$$

I_0 = Modified Bessel Function of first kind and first order,

$$\rho_0 = \frac{Z_2 - Z_1}{Z_2 + Z_1}$$

A = Magnitude of maximum allowable reflection in the pass band.

Using $\rho_0 = \frac{Z_2 - Z_1}{Z_2 + Z_1}$ however, causes discontinuities in the impedance

at $x = \pm l/2$ which can be avoided by using $\rho_0 = \frac{1}{2} \ln \left(\frac{Z_2}{Z_1} \right)$. The

Klopfenstein taper is exact in the limit that $\rho_0 \ll 1$, in which case either definition can be used. However, in this design, ρ_0 has a maximum value of 0.3, which introduces an additional 6% error in the evaluation of the characteristic impedance as a function of distance along the taper. The minimum length of the taper is obtained from the relation $\beta l > A$, where β is the wavevector at the lowest frequency of operation in that portion of the taper where the propagation velocity is smallest.

A taper designed as shown in Figure 5 will have an impedance at end A roughly half that at end E. Since the antenna radiation resistance must be restricted to 45Ω to keep its size small, it becomes impossible to transform the antenna impedance to that of a standard 50Ω flexible coax feed using just a single taper. As a result, two tapers are used; the first transforms the antenna impedance to an intermediate value of 25Ω using the technique illustrated in Figure 5, while the second transforms the impedance to 50Ω by gradually increasing the diameter of the inner conductor so that it is compatible with the coaxial feed at the other end.

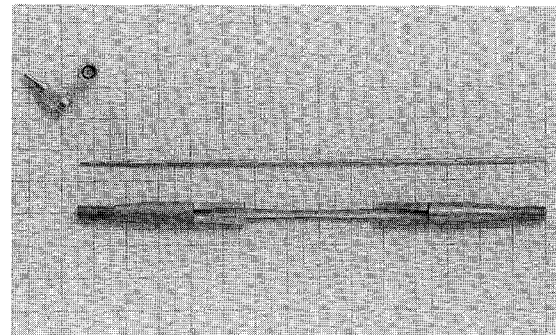


Figure 6: Back-to-back Balun Transformers

The design allowed 10% reflections at a minimum operating frequency of 4GHz and assumed that the entire balun was immersed in a medium with a relative permittivity of 2.25. This ensured compatibility with the teflon dielectric used in the flexible coaxial cable, minimizing reflections at the plug. Back-to-back baluns were fabricated as shown in Figure 6. The inner conductor was fabricated using center-less grinding while the outer one was made using Electric Discharge Machining. After assembly, the transformers were placed in a $1'' \times 1''$ cross-section mold which was filled with an epoxy and cured. The transformer pair was then bisected and the antenna flip-mounted on it using silver epoxy so that the two-wire end of the balun made good electrical contact with the two square pads of the antenna. The entire probe is shown in Figure 3.

The mechanical considerations satisfied by the design are rigidity, the ability to fit the probe flush with the plane of the substrate holder, longevity (metal accumulation on the probe is avoided due to back-side illumination) and vacuum compatibility. Since satisfying the last requirement meant finding an epoxy that would not outgas at high vacuum, we were forced to trade off high frequency loss with vacuum compatibility. X-Band tests on the epoxy used (Epon-812) showed its relative permittivity to be ~ 2 and the transmission loss in the balun was measured at $\sim 6\text{dB}$ at 8.2GHz. While an effort is underway to find a suitable epoxy that is less lossy in the 4-80GHz spectrum (over which the antenna is designed to radiate), we present only low frequency (4-4.5GHz) results in this paper.

Figure 7 shows the one-port return loss of the probe with "no load" (i.e., radiating into free space), an absorbing foam sheet and a thick steel plate placed over the antenna. The ~8dB return loss for case 1 (at 4.3GHz) is indicative of the power absorbed by the epoxy. Even without external tuning there is an average difference of ~5dB between cases 1 and 2 over the 500MHz range.

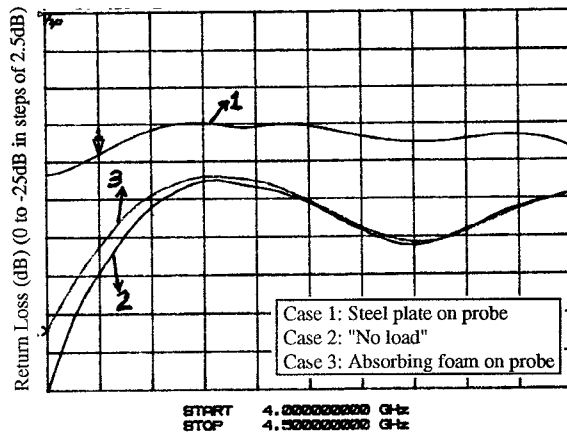


Figure 7: Return loss measurements on probe. The x-axis frequency scale is linear from 4.0 to 4.5GHz

Experimental results: Figure 8 shows the one port return loss with a 250 Ω -cm Si wafer used as the load. Three cases are shown: no film, a 0.2 μ m Al film and a 2.0 μ m Al film on the Si substrate.

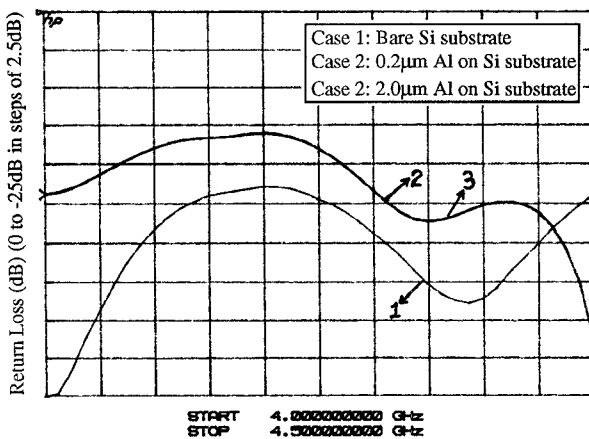


Figure 8: Return loss measurements (untuned) with Si wafer on probe. The x-axis frequency scale is linear from 4.0 to 4.5GHz

The 250 Ω -cm wafer is nearly "transparent" between 4 and 4.5GHz and the curves for the thin and thick Al films, as per the simulations, are indistinguishable. There is a ~5dB difference between case 1 and case 2, which can be enhanced to ~20dB with external tuning (Figure 9).

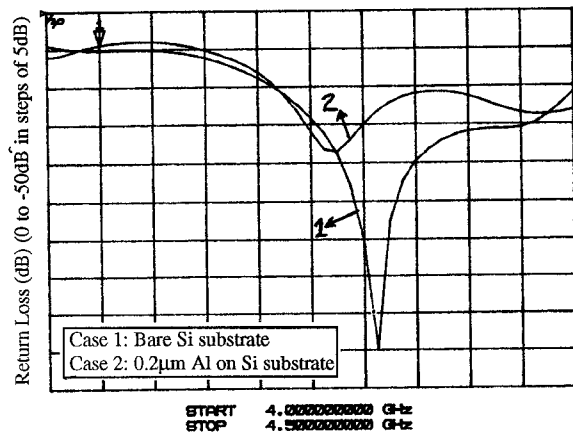


Figure 9: Return loss measurements (tuned) with Si wafer on probe. The x-axis frequency scale is linear from 4.0 to 4.5GHz

Conclusions: A microwave probe for measuring the thickness of conducting films has been fabricated and characterized. A difference of upto 20dB has been demonstrated between the two extrema of very small and infinitely large sheet resistivity for conducting films deposited on Si. Since the return loss will change by this amount as film thickness is increased from zero, simulation results indicate that the probe should be very effective in measuring the thickness of typical adhesion layers/diffusion barriers in VLSI and as an end-point detector in metal etching.

Acknowledgements: We acknowledge the support of the Center for Integrated Electronics for providing clean room support for the fabrication of the antennas and for providing equipment and material for Aluminum evaporation. We also thank Hemant Bhimnathwala for the Network Analyzer measurements and Dr. Yong Yun (M/A-COM) for providing the gold on GaAs sample. This work was partially supported by IBM, East Fishkill.

References

- [1] S. Wolf and R. N. Tauber, "Silicon Processing for the VLSI Era", Lattice Press, 1986.
- [2] John D. Dyson, "The Equiangular Spiral Antenna", IRE Transactions on Antennas and Propagation, Vol 6, p.210
- [3] J. W. Duncan and V. P. Minerva, "100:1 Bandwidth Balun Transformer", Proceedings of the IRE, Vol 48, p.156
- [4] R. W. Klopfenstein, "A Transmission Line Taper of Improved Design", Proceedings of the IRE, Vol 44, p. 31